Preparation and structural characterization of ruthenium(II) complexes of the peptides diglycine and triglycine

W. S. Sheldrick* and **R. Exner**

Lehrstuhl für Analytische Chemie, Ruhr-Universität Bochum, Postfach 10 21 48, W-4630 Bochum 1 (F.R.G.)

(Received December 3, 1990)

Abstract

The peptide complexes $[Ru(glyglyH_{-1})(PPh_3)_2(CH_3OH)]$ (**1**) and $[Ru(glyglyglyH_{-1})(PPh_3)_2]_2$ (**2**) may be prepared by the reaction of $[RuCl_2(PPh_3)_3]$ with diglycine (glyglyH) and triglycine (glyglyglyH), respectively, in methanol at reflux in the presence of base. Their molecular structures were established by X-ray analysis. **1** exhibits N(amino),N(peptide),O(carboxyl)-coordination of the central Ru atom. The PPh_3 ligands are positioned *trans* to a methanol oxygen and to a peptide nitrogen atom, respectively. In contrast, the triglycinate anion in **2** is tetradentate and displays N(amino),N(peptide),O(peptide),O(carboxyl')-coordination leading to the formation of a dimeric complex containing a 14-membered central ring system. The PPh_3 ligands are sited *trans* to a carboxyl oxygen and to a peptide nitrogen atom, respectively. The amino protons in **2** display a remarkable difference of 5.97 ppm in their respective signal positions in a ^1H NMR spectrum taken in CD_2Cl_2 solution. The electrochemistry of the dimeric complex **2** has been studied.

Introduction

The synthesis and structural characterization of a variety of organoruthenium(II) complexes of amino acidate ligands (aa) has been reported. Complexes of the type [(diene)Ru(aa)$_2$] (diene = norbornadiene nbd or 1,5-cyclooctadiene cod) may be prepared by the reaction of $[(diene)RuCl_2]_n$ with simple α-amino acids (aaH) such as glycine (glyH), D,L-alanine, (D,L-alaH), L-valine (L-valH) or L-phenylalanine (L-pheH) in aqueous solution at reflux [1, 2].

In contrast, the analogous reaction in methanol at reflux leads to the isolation of oligomeric complexes $[(diene)Ru(aa)]_n$ (aa = gly, D,L-ala, D,L-val, D,L-phe), in which the amino acidate ligand must be tridentate [2]. A crystal structure determination of tetrameric $[(cod)RuCl(D,L\text{-phe})]_4$ confirmed the presence of N(amino),O(carboxyl),O(carboxyl')-coordination, with symmetrical carboxyl bridges between individual ruthenium atoms. The reaction of $[(diene)RuCl_2]_n$ with the sulfur-containing amino acids D,L-methionine methyl ester (D,L-metme), D,L-methionine (D,L-metH) and D,L-penicillamine (D,L-penH) yielded the complexes $[(nbd)RuCl_2(D,L\text{-metme})]$, $[(nbd)RuCl(D,L\text{-met})]$ and $[(nbd)Ru(D,L\text{-penH}_{-1})]_2$ for which X-ray analyses established the amino acidate ligands as bi-, tri- and tetradentate, respectively, with S,N-, S,N,O- and S,S,N,O-coordination [3]. A similar preference for S and N coordination sites was also observed for (η^6-arene)ruthenium(II) complexes of L-penicillamine, L-histidine and triglycine (glyglyglyH) [4]. The latter compound $[(\eta^6\text{-}C_6H_6)RuCl(glyglygly)]$, which represents to our knowledge the only previously characterized peptide complex of ruthenium(II), displays N(amino), N(peptide)-coordination of the metal.

We have recently reported the synthesis and structural characterization of the (triphenylphosphine)ruthenium(II) complexes $[Ru(aa)_2(PPh_3)_2]$ (aa = gly, L-ala, L-val), in which the amino acidate ligands display N(amino),O(carboxyl)-coordination [5]. The reaction of $[RuCl_2(PPh_3)_3]$ with peptides should yield complexes in which these ligands are tri-, tetra- or even pentadentate. In this paper we present the synthesis and structural characterization of the peptide complexes $[Ru(glyglyglyH_{-1})(PPh_3)_2(CH_3OH)]$ (**1**) and $[Ru(glyglyglyH_{-1})(PPh_3)_2]_2$ (**2**) with tri- and tetradentate coordination of the bioligand, respectively. The peptide diglycine offers four potential metal binding sites, namely a carboxylate oxygen, a peptide nitrogen or oxygen atom and the terminal amino group. In the case of the tripeptide triglycine this range is extended, as

*Author to whom correspondence should be addressed.

0020-1693/91/$3.50

a result of the second peptide linkage, by a further peptide nitrogen and oxygen atom.

Experimental

All reactions were carried out under an inert gas atmosphere. Solvents were dried and distilled before use. IR spectra were recorded as 1% KBr discs on a Perkin-Elmer 297 spectrometer. NMR spectra were recorded on a Bruker AM 400 spectrometer at 20 °C. Cyclic voltammograms for **2** were measured at scan rates from 0.01 to 1 V s^{-1} for an approximate concentration of the electro-active component of 10^{-3} M. The complex was investigated in CH_2Cl_2 solution containing 0.1 M tetra-n-butylammonium hexafluorophosphate as supporting electrolyte at a glassy-carbon electrode and an Ag/AgCl reference electrode. The redox potentials were referenced versus the ferrocenium/ferrocene couple as internal standard [6]. Elemental analyses were performed with a Perkin-Elmer 240. The peptides diglycine and triglycine were purchased from Sigma Chemie GmbH and used as received. $RuCl_3 \cdot 3H_2O$ was a gift from Degussa AG. $[RuCl_2(PPh_3)_3]$ was prepared as described in the literature [7].

Preparation of complexes 1 and 2

$[Ru(glyglyH_{-1})(PPh_3)_2(CH_3OH)] \cdot 2CH_3OH$ (1)

A mixture of 282 mg (0.29 mmol) of $[RuCl_2(PPh_3)_3]$ and 42 mg (0.32 mmol) of diglycine was heated with stirring in the presence of 77 mg (0.33 mmol) Rb_2CO_3 for 2 h in 13 ml absolute methanol at reflux. The orange solution was filtered and allowed to cool to r.t. to yield crystals of **1**, which could be recrystallized from methanol. Yield 130 mg (53%).

$C_{43}H_{48}N_2O_6P_2Ru$ (*M* 851.9): *Anal.* Found: C, 60.7; H, 5.35; N, 3.4. Calc.: C, 60.62; H, 5.67; N, 3.29%. IR: 3000w, 2955w, ν(CH); 1605s, ν(CO) cm^{-1}. $^{31}P\{^1H\}$ NMR (d_4-methanol, external 85% H_3PO_4 standard): 53.66 (s, broad, 1P), 33.39 (s, broad, 1P) ppm. ^1H NMR (d_4-methanol, TMS) 2.70, 2.90 (2m, 4H glyglyH$_{-1}$ CH_2), 7.12–7.64 (mm, 30H, Ph–H) ppm.

$[Ru(glyglyglyH_{-1})(PPh_3)_2]_2 \cdot 6CH_3OH$ (2)

A mixture of 274 mg (0.28 mmol) of $[RuCl_2(PPh_3)_3]$ and 55 mg (0.29 mmol) of triglycine was heated with stirring in the presence of 0.62 ml 1 M NaOMe for 3 h in 40 ml absolute methanol at reflux. The solvent volume was reduced to 5 ml and the solution left to crystallize at −30 °C to yield orange–yellow crystals of **2**. Yield 130 mg (60%). Suitable crystals for an X-ray structural analysis were obtained by recrystallization from C_2H_5OH/CH_2Cl_2 solution.

$C_{87}H_{90}N_6O_{11}P_4Ru_2$ (*M* 1721.7): *Anal.* Found: C, 60.3; H, 4.80; N, 5.1. Calc.: C, 60.69; H, 5.27; N, 4.89%. IR: 3390m, ν(NH); 3270w, 3220w, $\nu(NH_2)$; 1600s, ν(CO), 1595s, $\delta(NH_2)$ cm^{-1}. $^{31}\{^1H\}$ NMR (CD_2Cl_2, external 85% H_3PO_4 standard): 62.32 (d, 1P, $^2J(PP) = 31$ Hz), 44.37 (d, 1P) ppm. ^1H NMR (CD_2Cl_2, TMS) 1.62, 7.59 (2m, 4H, NH_2(amino)), 1.81, 3.50 (2d, 4H, $^2J(HH) = 19.8$ Hz, C(O)–CH_2–N-(peptide)), 2.48 (m, 2H, CH–N(amino)), 3.02 (m, 2H, CH–N(amino)), 2.20 (dd, 2H, CH–N–(peptide)), 4.02 (m, 2H, CH–N(peptide)), 3.84 (dd, 2H, NH(peptide)), 6.8–7.7 (mm, 60H, Ph–H) ppm.

X-ray structural analyses of 1 and 2

Crystal and refinement data are summarized in Table 1. The asymmetric unit of **1** contains two methanol solvate molecules, that of **2** three ethanol solvate molecules. Unit cell constants were obtained from a least-squares fit to the settings of 25 reflections centered on an Enraf-Nonius CAD4 diffractometer. Intensities were collected on the diffractometer in the ω-mode at speeds varying between 0.91 nd 5.09° min^{-1} for **1** and 0.96 and 6.71° min^{-1} for **2**. Graphite-monochromated Mo Kα-radiation was employed for a crystal of dimensions $0.60 \times 0.32 \times 0.30$ mm in the case of **1**. For the smaller crystal of **2** ($0.42 \times 0.23 \times 0.16$ mm) Cu Kα-radiation was used for the data collection. Empirical absorption corrections were applied to the reflection intensities. The structures were solved by Patterson syntheses and refined by full-matrix least-squares. A difference synthesis revealed the positions of four disordered methanol solvate molecules in the asymmetric unit of **1**. These were assigned site occupation factors of 0.5 and refined with joint isotropic temperature factors for the carbon and oxygen atoms of individual molecules. Anisotropic temperature factors were introduced for all non-hydrogen atoms of the complex **1**. Hydrogen atoms were included at geometrically calculated positions with group isotropic temperature factors.

In the case of complex **2** a difference synthesis indicated the presence of three ethanol solvate molecules in the asymmetric unit. Although these were found to exhibit relatively high isotropic temperature factors (Table 2) an analysis of their network of O–H...O and O–H...N hydrogen bonds in the crystal lattice suggested full site occupation. The remaining non-hydrogen atoms of **2** were refined anisotropically. Hydrogen atoms in the complex were included at geometrically calculated sites and assigned group isotropic temperature factors.

Terminal reliability indices are listed in Table 1, where $R_w = [\Sigma w(F_o - F_c)^2 / \Sigma w F_o^2]^{1/2}$, with weights given by the expression $w = [\sigma^2(F_o) + p^2 F_o^2]^{-1}$. Values of p are given in Table 1. Calculations were performed

TABLE 1. Crystal and refinement data

Compound	1	2
Formula	$[Ru(glyglyH_{-1})(PPh_3)_2(CH_3OH)]\cdot 2CH_3OH$	$[Ru(glyglyglyH_{-1})(PPh_3)_2]_2\cdot 6C_2H_5OH$
Space group	$P\bar{1}$	$P2_1/c$
a (Å)	14.613(4)	16.513(2)
b (Å)	16.051(4)	17.550(2)
c (Å)	12.411(3)	17.310(2)
α (°)	93.22(3)	90
β (°)	104.25(4)	107.00(1)
γ (°)	114.57(2)	90
V (Å^3)	2524(3)	4797(2)
Z	2	2
M	851.9	1902.1
D_c (g cm^{-3})	1.12	1.32
Radiation	Mo Kα	Cu Kα
μ (cm^{-1})	4.1	37.5
Scan method	ω	ω
$2\theta_{max}$ (°)	45	115
Reflections measured	5628	6926
Reflections observed	4058	5377
Rejection criterion	$F_o^2 < 2\sigma(F_o^2)$	$F_o^2 < 2\sigma(F_o^2)$
R	0.068	0.062
R_w	0.068	0.062
p	0.014	0.014

with SHELX [8] and with local programs. The molecular structures in Figs. 1 and 2 were drawn with RSPLOT [9]. Atom positional parameters with equivalent isotropic temperature factors are listed in Table 2, bond distances and angles to the ruthenium atoms in Table 3.

Discussion

The molecular structure of $[Ru(glyglyH_{-1})(PPh_3)_2(CH_3OH)]$ (**1**) is depicted in Fig. 1. Both chloride ligands are substituted in the reaction between $[RuCl_2(PPh_3)_3]$ and diglycine, although this was carried out in the presence of Rb_2CO_3. The formation of the neutral methanol adduct rather than the alternative complex anion $[RuCl(glyglyH_{-1})(PPh_3)_2]^-$ is obviously favoured under the conditions chosen. Complex **1** exhibits N(amino),N(peptide),O(carboxyl)-coordination of the central ruthenium atom Ru1. The PPh_3 ligands are sited *trans* to the methanol oxygen and to the peptide nitrogen atom, respectively. As complex **1** crystallizes in the centrosymmetric space group $P\bar{1}$ both Ru_R and Ru_S enantiomers are present in the unit cell.

In an early review [10], Freeman concluded that when a metal ion is bonded to three donor groups of a peptide molecule, the central one of which is a peptide nitrogen, then the three donor atoms and the metal must be almost coplanar. This is the state of affairs for the atoms N2, N1, O1 and Ru1 in complex **1**. Although this mode of peptide coordination has not, to our knowledge, been previously reported for a group 8 metal ion, analogous examples are known for members of the neighbouring groups 9 and 10, e.g. in $[Co^{II}(H_2O)_6][D,L\text{-}Co^{III}(glyglyH_{-1})_2]_2$ [11], $[D,L\text{-}Co^{III}(glygly)_2][ClO_4]$ [11] and $Na_2[Ni(glyglyH_{-1})_2]\cdot 8H_2O$ [12]. The Ru–O distance to the donor methanol oxygen atom is, as expected, markedly longer (2.204(6) Å) than that to the carboxyl oxygen (2.096(7) Å). A similar difference is also observed for the Ru–N bond distances to the donor amino nitrogen (2.131(7) Å) and to the peptide nitrogen (2.016(8) Å). A marked *trans* influence on the Ru–P bond lengths in **1** is apparent. Whereas the Ru1–P2 bond *trans* to the Ru1–N1(peptide) bond displays a distance of 2.341(3) Å, the Ru1–P1 bond *trans* to Ru1–O10(methanol) is 0.092 Å shorter. The $^{31}P\{^1H\}$ NMR spectrum contains an AB system for the magnetically inequivalent phosphorus atoms P1 and P2. As the degree of d_π–p_π backbonding to P1 must be significantly greater than to P2, a relative deshielding of the latter phosphorus would be expected. It is, therefore, possible to perform an assignment of the lowfield resonance at 53.66 ppm to P2 and the highfield resonance at 33.39 ppm to P1.

The disordered methanol solvate molecules in the crystal lattice of **1** participate in a complicated network of O–H...O and O–H...N hydrogen bonds involving O1, N2 and O10.

TABLE 2. Atom positional parameters with equivalent isotropic temperature factors (Å$\times 10^3$)

Atom	x/a	y/b	z/c	U_{eq}[a]
Compound **1**				
Ru1	0.9567(1)	0.1435(1)	0.3135(1)	57(1)
P1	0.9574(2)	0.2755(2)	0.3858(2)	67(1)
P2	0.8322(2)	0.1091(5)	0.1370(2)	68(1)
O1	1.0968(6)	0.2221(5)	0.2759(6)	73(4)
O2	1.2683(7)	0.2693(6)	0.3365(7)	117(5)
O3	1.0935(6)	0.1067(4)	0.6285(6)	74(4)
N1	1.0651(6)	0.1514(6)	0.4555(7)	59(4)
N2	0.8575(6)	0.0522(5)	0.3991(6)	57(4)
C1	1.1775(11)	0.2290(8)	0.3510(12)	83(7)
C2	1.1735(8)	0.1924(8)	0.4590(9)	71(6)
C3	1.0349(8)	0.1138(7)	0.5366(10)	62(5)
C4	0.9172(8)	0.0748(7)	0.5222(8)	60(5)
C112	0.8880(6)	0.3422(5)	0.5460(7)	80(6)
C113	0.8116(6)	0.3405(5)	0.5957(7)	109(8)
C114	0.7093(6)	0.2687(5)	0.5558(7)	123(10)
C115	0.6835(6)	0.1986(5)	0.4662(7)	103(8)
C116	0.7600(6)	0.2003(5)	0.4165(7)	78(6)
C111	0.8622(6)	0.2721(5)	0.4563(7)	68(6)
C122	0.8984(7)	0.4102(6)	0.2966(7)	103(8)
C123	0.8970(7)	0.4710(6)	0.2209(7)	135(10)
C124	0.9517(7)	0.4801(6)	0.1412(7)	157(12)
C125	1.0079(7)	0.4285(6)	0.1373(7)	146(11)
C126	1.0093(7)	0.3677(6)	0.2129(7)	109(8)
C121	0.9546(7)	0.3585(6)	0.2926(7)	86(7)
C132	1.0965(8)	0.3218(5)	0.6039(9)	81(6)
C133	1.1945(8)	0.3695(5)	0.6852(9)	109(8)
C134	1.2765(8)	0.4413(5)	0.6595(9)	154(12)
C135	1.2605(8)	0.4654(5)	0.5526(9)	157(12)
C136	1.1624(8)	0.4176(5)	0.4713(9)	109(8)
C131	1.0804(8)	0.3458(5)	0.4970(9)	72(6)
C212	0.9790(7)	0.1969(6)	0.0244(7)	94(7)
C213	1.0117(7)	0.2354(6)	−0.0654(7)	122(9)
C214	0.9392(7)	0.2416(6)	−0.1577(7)	136(11)
C215	0.8340(7)	0.2093(6)	−0.1601(7)	134(11)
C216	0.8013(7)	0.1708(6)	−0.0703(7)	107(8)
C211	0.8738(7)	0.1646(6)	0.0219(7)	78(6)
C222	0.7775(6)	−0.0422(6)	−0.0355(7)	87(7)
C223	0.7432(6)	−0.1360(6)	−0.0778(7)	110(8)
C224	0.7087(6)	−0.2030(6)	−0.0113(7)	119(9)
C225	0.7088(6)	−0.1762(6)	0.0976(7)	116(9)
C226	0.7432(6)	−0.0825(6)	0.1400(7)	96(7)
C221	0.7776(6)	−0.0155(6)	0.0734(7)	67(5)
C232	0.6218(9)	0.0502(6)	0.1362(8)	127(9)
C233	0.5339(9)	0.0646(6)	0.1358(8)	180(14)
C234	0.5373(8)	0.1520(6)	0.1269(8)	194(16)
C235	0.6285(9)	0.2251(6)	0.1185(8)	163(12)
C236	0.7164(9)	0.2107(6)	0.1190(8)	116(9)
C231	0.7131(9)	0.1233(6)	0.1278(8)	88(7)
O10	0.9812(5)	0.0225(4)	0.2623(5)	72(4)
C10	1.0279(10)	0.0077(8)	0.1780(10)	94(7)
O100	0.6261(20)	−0.0532(18)	0.3768(21)	180(8)*
C100	0.5483(26)	−0.1363(22)	0.3059(29)	180(8)*
O200	0.5519(16)	−0.2699(14)	0.5951(17)	145(6)*
C200	0.4992(24)	−0.2999(21)	0.6760(23)	145(6)*
O300	0.6909(18)	0.5986(16)	−0.1908(29)	163(7)*
C300	0.6520(27)	0.5305(21)	−0.2876(24)	163(7)*
O400	0.6374(21)	−0.0626(18)	0.5544(23)	196(9)*
C400	0.6676(31)	−0.0031(26)	0.6568(27)	196(9)*

(*continued*)

TABLE 2. (*continued*)

Atom	x/a	y/b	z/c	U_{eq}[a]
Compound **2**				
Ru1	0.3082(1)	0.5416(1)	0.3588(1)	34(1)
P1	0.2903(1)	0.4159(1)	0.3101(1)	37(1)
P2	0.1749(1)	0.5662(1)	0.3647(1)	40(1)
O1	0.5576(3)	0.4791(2)	0.6248(3)	40(2)
O2	0.5221(3)	0.3968(3)	0.7088(3)	63(3)
O3	0.3480(3)	0.5169(3)	0.4848(3)	40(2)
O5	0.3543(3)	0.7741(3)	0.3832(3)	60(3)
N1	0.4164(3)	0.5638(3)	0.6073(3)	44(3)
N2	0.3467(3)	0.6456(3)	0.4075(3)	40(3)
N3	0.3028(3)	0.6077(3)	0.2546(3)	37(3)
C1	0.5089(4)	0.4512(4)	0.6619(4)	44(4)
C2	0.4229(4)	0.4897(4)	0.6471(4)	51(4)
C3	0.3820(4)	0.5723(4)	0.5282(5)	41(4)
C4	0.3853(4)	0.6506(4)	0.4934(4)	43(4)
C5	0.3359(4)	0.7055(4)	0.3596(5)	46(4)
C6	0.2957(4)	0.6882(4)	0.2721(4)	46(4)
C112	0.1160(3)	0.3911(3)	0.2387(3)	71(5)
C113	0.0447(3)	0.3633(3)	0.1804(3)	79(6)
C114	0.0541(3)	0.3233(3)	0.1139(3)	75(5)
C115	0.1346(3)	0.3112(3)	0.1057(3)	93(7)
C116	0.2059(3)	0.3390(3)	0.1640(3)	76(6)
C111	0.1965(3)	0.3790(3)	0.2305(3)	45(4)
C122	0.3934(3)	0.4330(2)	0.2095(3)	50(4)
C123	0.4548(3)	0.4111(2)	0.1732(3)	65(5)
C124	0.4964(3)	0.3415(2)	0.1931(3)	70(5)
C125	0.4766(3)	0.2937(2)	0.2494(3)	69(5)
C126	0.4152(3)	0.3156(2)	0.2858(3)	53(4)
C121	0.3735(3)	0.3852(2)	0.2656(3)	43(4)
C132	0.3711(3)	0.3543(2)	0.4590(3)	49(4)
C133	0.3860(3)	0.3013(2)	0.5217(3)	65(5)
C134	0.3330(3)	0.2383(2)	0.5150(3)	81(6)
C135	0.2650(3)	0.2282(2)	0.4456(3)	86(6)
C136	0.2500(3)	0.2812(2)	0.3829(3)	66(5)
C131	0.3031(3)	0.3442(2)	0.3896(3)	39(3)
C212	0.1662(3)	0.4430(3)	0.4622(3)	63(5)
C213	0.1255(3)	0.3874(3)	0.4950(3)	82(6)
C214	0.0375(3)	0.3812(3)	0.4685(3)	109(8)
C215	−0.0099(3)	0.4306(3)	0.4092(3)	106(5)
C216	0.0308(3)	0.4861(3)	0.3764(3)	74(5)
C211	0.1188(3)	0.4923(3)	0.4029(3)	45(4)
C222	0.1864(3)	0.6243(2)	0.5193(3)	53(4)
C223	0.1939(3)	0.6819(2)	0.5765(3)	67(5)
C224	0.1911(3)	0.7581(2)	0.5530(3)	71(5)
C225	0.1808(3)	0.7767(2)	0.4724(3)	68(5)
C226	0.1733(3)	0.7191(2)	0.4152(3)	55(4)
C221	0.1761(3)	0.6429(2)	0.4387(3)	44(4)
C232	0.1018(3)	0.5785(3)	0.1982(3)	64(5)
C233	0.0447(3)	0.6065(3)	0.1277(3)	94(7)
C234	−0.0195(3)	0.6564(3)	0.1324(3)	120(8)
C235	−0.0266(3)	0.6782(3)	0.2076(3)	113(7)
C236	0.0304(3)	0.6503(3)	0.2781(3)	83(6)
C231	0.0946(3)	0.6004(3)	0.2735(3)	53(4)
O100	0.2608(5)	0.5616(4)	0.0777(4)	117(5)*
O200	0.3772(7)	0.6417(6)	0.0218(6)	176(8)*
O300	0.2419(9)	0.6169(8)	0.7896(8)	254(11)*
C101	0.2480(10)	0.4954(8)	0.0223(10)	191(5)*
C102	0.1544(10)	0.4975(10)	−0.0190(10)	191(5)*
C201	0.4603(11)	0.6480(15)	0.0844(11)	276(8)*
C202	0.5176(13)	0.6056(14)	0.0465(14)	276(8)*
C301	0.2903(13)	0.5471(12)	0.7946(15)	24(7)*
C302	0.2226(14)	0.4899(13)	0.7476(13)	244(7)*

[a]Starred atoms were refined anisotropically.

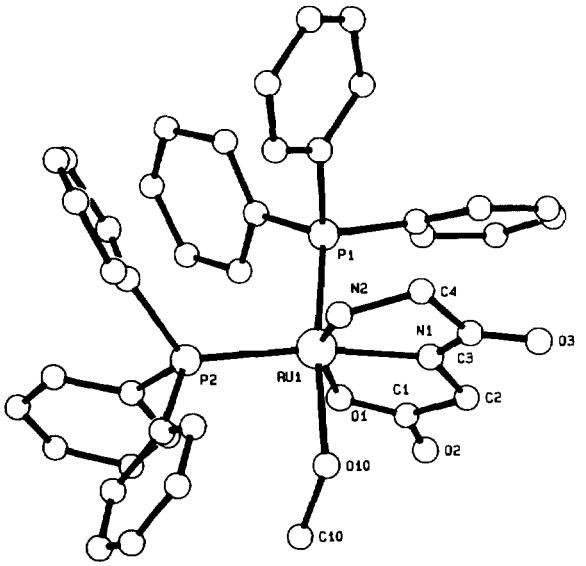

Fig. 1. Molecular structure of $[Ru(glyglyH_{-1})(PPh_3)_2(CH_3OH)]$ (1).

Reaction of $[RuCl_2(PPh_3)_3]$ with triglycine in methanol also leads to the substitution of both chloride ligands and to the loss of one PPh_3 ligand. As a result of the availability of two further potential metal binding sites in comparison to diglycine, the peptide anion in $[Ru(glyglyglyH_{-1})(PPh_3)_2]_2$ (2) is able to occupy all four vacant positions in the octahedral coordination sphere of the ruthenium atom Ru1 (Fig. 2). The N(amino),N(peptide),O(peptide),O(carboxyl')-coordination exhibited by 2 leads to the formation of a dimeric complex with crystallographic C_i symmetry. Although, this particular binding mode has not, to our knowledge, been previously observed for a metal–peptide complex, O(peptide)-coordination has been found in several tripeptide complexes, e.g. $[Cu(glyleutyr)]\cdot 8H_2O\cdot(C_2H_5)_2O$ [13] and $[Zn(glyglygly)(H_2O)_2]_2[SO_4]\cdot 4H_2O$ [14]. The observation of O(peptide)-coordination in 2 was unexpected. If the basicities of the potential binding sites in the triglycine ligand are compared then the formation of a Ru1–N1(peptide) bond rather than a Ru1–O3(peptide) bond would be predicted. This would also have been in accordance with our previous finding that S and N coordination sites are preferred for the relatively soft ruthenium(II) centres [3, 4]. However, inspection of Fig. 2 indicates that Ru1–N1(peptide) binding would lead to sterically unfavourable preconditions for the formation of a Ru1–O1(carboxyl) bond in either a monomeric or a dimeric complex.

The amino nitrogen N3 is displaced 0.461 Å from the best least-squares plane through the atoms of the bichelate ring system. A similar displacement of 0.457 Å was observed for the amino nitrogen N2 in 1. As a result of the formation of the Ru1–O3 bond, the C3–O3 distance in 2 is lengthened to 1.257(8) Å. This compound also displays the typical shortening

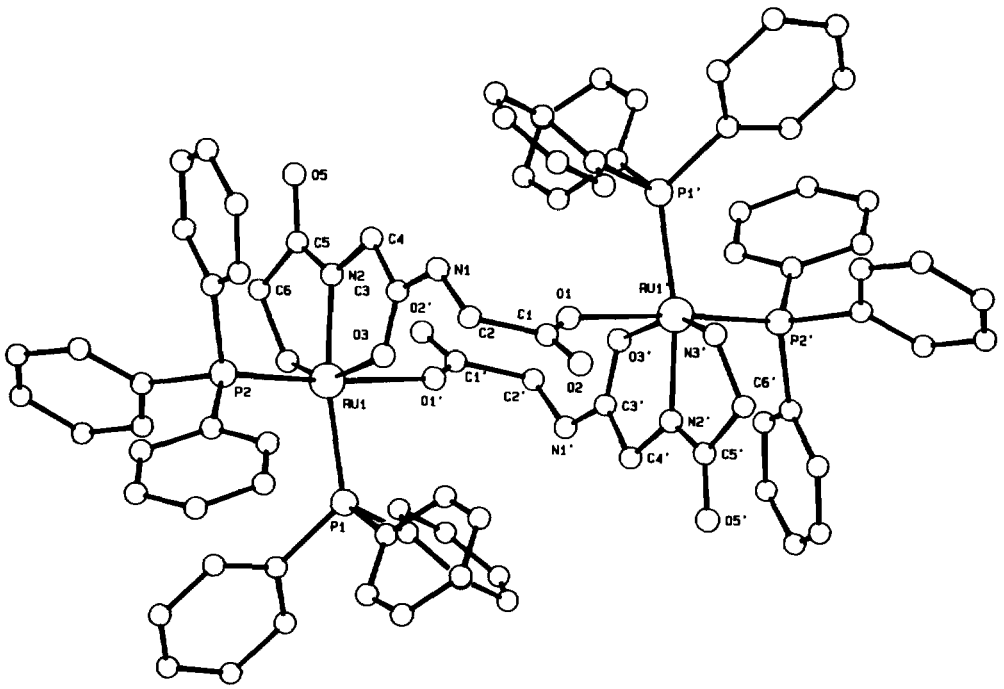

Fig. 2. Molecular structure of $[Ru(glyglyglyH_{-1})(PPh_3)_2]_2$ (2).

TABLE 3. Bond distances (Å) and angles (°) to the ruthenium atoms in **1** and **2**

1			
Ru1–P1	2.249(3)	Ru1–P2	2.341(3)
Ru1–O1	2.096(7)	Ru1–N1	2.016(8)
Ru1–N2	2.131(7)	Ru1–O10	2.204(6)
P1–Ru1–P2	99.3(1)	O1–Ru1–P1	89.9(2)
O1–Ru1–P2	101.0(2)	N1–Ru1–P1	91.3(2)
N1–Ru1–P2	169.4(2)	N1–Ru1–O1	78.9(3)
N2–Ru1–P1	97.4(2)	N2–Ru1–P2	99.0(2)
N2–Ru1–O1	157.3(3)	N2–Ru1–N1	79.5(3)
O10–Ru1–P1	170.8(2)	O10–Ru1–P2	89.2(2)
O10–Ru1–O1	85.0(3)	O10–Ru1–N1	80.3(3)
O10–Ru1–N2	84.6(3)		
2			
Ru1–P1	2.350(2)	Ru1–P2	2.275(2)
Ru1–O1′	2.181(5)	Ru1–O3	2.130(5)
Ru1–N2	2.031(5)	Ru1–N3	2.124(5)
P1–Ru1–P2	99.9(1)	O3–Ru1–P1	98.3(1)
O3–Ru1–P2	90.3(1)	N2–Ru1–P1	169.5(2)
N2–Ru1–P2	90.0(2)	N2–Ru1–O3	78.0(2)
N3–Ru1–P1	103.8(1)	N3–Ru1–P2	97.7(1)
O1′–Ru1–P1	84.6(1)	O1′–Ru1–P2	170.3(2)
N3–Ru1–O3′	154.8(2)	N3–Ru1–N2	78.1(2)
N3–Ru1–O1′	89.5(2)	N2–Ru1–O1′	85.0(2)
O3–Ru1–O1′	80.5(2)		

of the C–N bonds (N1–C3 1.328(8), N2–C5 1.319(8) Å) and lengthening of the non-coordinated C–O bond (C5–O5 1.257(8) Å) for a metal–peptide complex [10]. As for **1**, marked differences in the Ru–N, Ru–O and Ru–P bond lengths are also exhibited by complex **2**. However, whereas the difference between the Ru1–N3(amino) and Ru1–N2(peptide) bonds (2.130(5) and 2.031(5) Å, respectively) is similar to that in **1**, this is not the case for the Ru–O bonds. Surprisingly the dative Ru1–O3(peptide) bond (2.130(5) Å) is markedly shorter than the Ru1–O1′(carboxyl) bond. This latter bond is lengthened by 0.085–2.181(5) Å in comparison to the analogous Ru1–O1(carboxyl) bond in **1**, which, of course, is a member of a chelate ring system. A marked *trans* influence on the Ru–P bond lengths is once again apparent. The Ru–P bond *trans* to the Ru–N(peptide) bond is 0.075 Å longer than that *trans* to the Ru–O(carboxyl) bond (Ru1–P1 2.350(2) Å, Ru1–P2 2.275(2) Å). It may be assumed that the degree of d_π–p_π backbonding to P2 will be significantly greater than to P1, so that a relative deshielding of the latter phosphorus atom would be predicted. The $^{31}P\{^1H\}$ NMR spectrum contains an AB system with resonances at 62.32 and 44.37 ppm, which may be assigned to P1 and P2, respectively.

The dimeric complex **2** exhibits a central metallocyclic ring system with 14 member atoms (Fig. 2). Two symmetry related O1...H–N3′ hydrogen bonds of length 2.775 Å (O2...H 1.90 Å) stabilize the observed conformation of the complex in the crystal lattice. NMR studies indicate that C_i symmetry and a rigid central ring system are retained in CD_2Cl_2 solution. An assignment of the individual resonances in the ^1H NMR spectrum (CD_2Cl_2 solution) depicted in Fig. 3 was possible with the help of H, C and H, H COSY spectra. Resonances of the methylene C2 protons, which couple with the N1 peptide proton (p, 3.84 ppm), are observed at 2.20 (y) and 4.02 (y′) ppm. The C4 protons (x, x), which display only geminal coupling ($^2J(HH) = 19.8$ Hz), give rise to signals at 1.81 and 3.50 ppm. The amino N3 protons (a, a′) display a remarkable difference of 5.97 ppm in their respective resonance positions of 1.62 and 7.59 ppm. These protons couple with the C6 methylene protons, which are observed at 2.48 (z) and 3.02 (z′) ppm. As may be seen from Fig. 2, the environments of the N3 amino protons differ considerably from one another. Whereas one proton (presumably a′) participates in the relatively strong intramolecular N3–Ha′...O2 hydrogen bond, which may be assumed to continue to exist in CD_2Cl_2 solution, the other proton (presumably a) may possibly be influenced by the ring current of an adjacent phenyl ring. A short Ha...C232 distance of 2.40 Å (Ha...H232 1.79 Å) is observed to one of the P2 phenyl rings.

In view of the presence of two ruthenium(II) atoms in the dimeric complex **2**, it appeared to us to be of interest to study the redox behaviour of this complex. In the potential range −0.2 to +0.9 V versus Ag/AgCl, **2** shows two one-electron transfer waves lying very close to one another at approximately 0.02 and 0.11 V versus Fc^+/Fc (average value 0.07 V versus Fc^+/Fc). As the potential difference is less than 0.1 V it is not possible to resolve the individual

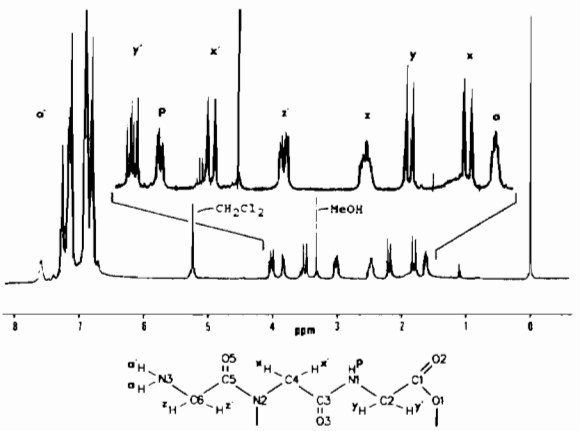

Fig. 3. ^1H NMR spectrum of **2** in CD_2Cl_2 solution with a resonance assignment on the basis of H, C and H, H COSY spectra.

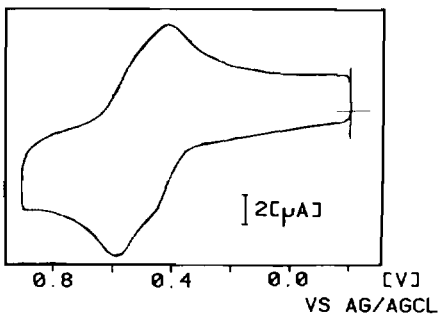

Fig. 4. Cyclic voltammogram of **2** (CH_2Cl_2; 0.1 M [n-Bu_4N]PF_6) at a glassy-carbon electrode (scan speed 0.4 V s^{-1}).

waves (Fig. 4). At scan speeds greater than 0.1 V s^{-1} characteristic values of I_p^A/I_p^C and ΔE_p for a reversible system are obtained. It seems reasonable to assume that an intermediate Ru(II),Ru(III) complex is formed during the oxidation of the Ru(II), Ru(II) complex **2** to a dicationic Ru(III),Ru(III) species.

Acknowledgements

This work was supported by the Fonds der Chemischen Industrie, Frankfurt. We are grateful to Professor Dr K. Wieghardt (Bochum) for the measurement of the cyclic voltammograms and to Degussa AG, Hanau, for a gift of $RuCl_3 \cdot 3H_2O$.

References

1 C. Potvin, L. Davignon and G. Pannetier, *Bull. Soc. Chem. Fr.*, (1974) 507.
2 W. S. Sheldrick and R. Exner, *Inorg. Chim. Acta, 166* (1989) 213.
3 W. S. Sheldrick and R. Exner, *J. Organomet. Chem., 386* (1990) 375.
4 W. S. Sheldrick and S. Heeb, *J. Organomet. Chem., 377* (1989) 357.
5 W. S. Sheldrick and R. Exner, *Inorg. Chim. Acta, 175* (1990) 261.
6 H. M. Koepp, H. Wendt and H. Strehlow, *Z. Elektrochem., 64* (1960) 483.
7 P. S. Hallman, T. A. Stephenson and G. Wilkinson, *Inorg. Synth., 12* (1970) 237.
8 G. M. Sheldrick, *SHELX-76,* computer program for crystal structure determination, University of Cambridge, U.K., 1976.
9 W. S. Sheldrick, *RSPLOT*, a computer program for molecule and lattice plots, TU Braunschweig, F.R.G., 1975.
10 H. C. Freeman, *Adv. Protein Chem., 22* (1967) 257.
11 M. T. Barnet, H. C. Freeman, D. A. Buckingham, I.-N. Hsu and D. Van der Helm, *J. Chem. Soc., Chem. Commun.*, (1970) 387.
12 H. C. Freeman and J. M. Guss, *Acta Crystallogr., Sect. B, 34* (1978) 2451.
13 W. A. Franks and D. Van der Helm, *Acta Crystallogr., Sect. B, 27* (1971) 1299.
14 D. Van der Helm and H. B. Nicholas, *Acta Crystallogr., Sect. B, 26* (1970) 367.